Dip-bump structure of the elastic hadron-hadron differential cross section

M. Kawasaki*
Physics Department, Gifu University, Yanagido, Gifu 501-1193, Japan

T. Maehara†
Graduate School of Education, Hiroshima University, Higashi-Hiroshima 739-8524, Japan

M. Yonezawa‡
Department of Environment and Information Science, Fukuyama University, Fukuyama 729-0292, Japan
(Received 11 August 2002; published 21 January 2003)

For elastic hadron-hadron diffraction scattering, we examine the relation between the zeros of the scattering amplitude and the zeros of the Fourier-Bessel-transformed eikonal function from the impact-parameter space to the momentum-transfer space. Any zero of the transformed eikonal function produces a zero trajectory which becomes confluent with the one of the black-disk amplitude as the energy goes higher.

DOI: 10.1103/PhysRevD.67.014013 PACS number(s): 13.85.Dz, 12.40.Nn

I. INTRODUCTION

Much effort has been devoted to the study of the diffraction interactions by quantum chromodynamics which is the fundamental theory of the strong interaction [1], but a detailed clarification of this interaction has not been attained yet. We consider it still useful to make phenomenological studies along with those of the basic theory.

The dip-bump structure of the differential cross section of elastic hadron-hadron scattering is a characteristic signature of diffraction scattering. We observe such dip-bump structures in pp and $\bar{p}p$ scattering in the energy region of the CERN Intersecting Storage Rings (ISR) and some symptoms of such structures also for meson-baryon scattering of which experiments are available only at sub-ISR energies. The diffraction pattern of the differential cross section is produced by the zeros of the scattering amplitude. In this paper we discuss the question of whether these zeros emerge *singly* or *in pairs*. This simple question seems to have been given no clear answer, either theoretically or experimentally.

II. BASIC FORMULAS

We assume the dominance of the imaginary part of the crossing even amplitude for the diffraction scattering in the following analysis; hence, we do not distinguish between hadron-hadron scattering and antihadron-hadron scattering. Let us take the impact-parameter representation of the imaginary part of the scattering amplitude, $\mathrm{Im}\,F(s,t)$ as

$$\mathrm{Im}\,F(s,t)=\int_0^\infty (1-e^{-\Omega(s,b)})J_0(\sqrt{-t}b)bdb, \qquad (1)$$

where s is the squared total energy in the center-of-mass system, t the squared momentum transfer, b the impact parameter, J_0 the Bessel function of order zero, and Ω the real eikonal function. Here the scattering amplitude $F(s,t)$ is normalized to give the differential cross section as

$$\frac{d\sigma}{dt}=\pi|F(s,t)|^2. \qquad (2)$$

The real part of the scattering amplitude is not considered in the present analysis. The real part tends to mask the dip structure arising from the imaginary part in the differential cross section and in the quantitative analysis of the experimental data it has to be included. If it is required, we can introduce it by the derivative dispersion relation [2].

In the eikonal model approach the eikonal function $\Omega(s,b)$ is related to the hadron dynamics. It is sometimes more appropriate to discuss the Fourier-Bessel-transformed eikonal function $\bar{\Omega}(s,t)$ from impact-parameter space to momentum-transfer space rather than the eikonal function $\Omega(s,b)$ itself. This is defined by

$$\bar{\Omega}(s,t)=\int_0^\infty \Omega(s,b)J_0(\sqrt{-t}b)bdb. \qquad (3)$$

In the following we refer to $\bar{\Omega}(s,t)$ as the t-eikonal function when we distinguish it specifically from $\Omega(s,b)$.

The zeros of the scattering amplitude, which is going to produce the dip-bump structure of the differential cross section, are induced in the framework of the eikonal picture either (i) by the zeros *inherent* in the t-eikonal function $\bar{\Omega}(s,t)$ or (ii) by the higher order effects of the eikonal function generated by the exponentiation of the eikonal function $\Omega(s,b)$ as in Eq. (1). It is clear that the zeros of the scattering amplitude are created in pairs in the latter case [3].

As for pp scattering, which shows a distinct dip-bump structure of the differential cross section in the ISR energy region, the scattering in the small momentum-transfer region up to the dip-bump structure can be well described either by the positive-definite t-eikonal function or by the one having zero. The representative of the former type of eikonal func-

*Email address: kawasaki@cc.gifu-u.ac.jp
†Email address: tmaehar@hiroshima-u.ac.jp
‡Email address: yonezawa@fuhc.fukuyama-u.ac.jp

tion is the classical Chou-Yang (CY) model where the *t*-eikonal function is given by the product of the absorptive matter distribution form factors of two hadrons and hence is positive definite for pp and $\bar{p}p$ scattering [4]. This type of model having a positive-definite *t*-eikonal function, however, has the difficulty of the appearance of a secondary dip against the experimental data, associated with the first one, if we extend the applicability of the model beyond the first dip-bump region. In fact we would have a secondary dip at $|t| \approx 4$ $(\mathrm{GeV}/c)^2$ at the ISR energy region for the *t*-eikonal function given by the product of dipole form factors.

This difficulty can be overcome if the *t*-eikonal function has a simple zero in the momentum transfer t [5] and the model given by Bourrely, Soffer, and Wu (BSW) [6] has such an amplitude. A careful study of this problem has been made for the experimental data of pp scattering at $23.5 \leqslant \sqrt{s} \leqslant 62.5$ GeV and the existence of a zero at $|t| = 7.0 \pm 2.0$ $(\mathrm{GeV}/c)^2$ has been concluded by Carvalho and Menon [7]. This zero can be interpreted in a sense as developing into the first dip of the pp differential cross section at $|t| \approx 1.4$ $(\mathrm{GeV}/c)^2$ in the ISR region. Here we should stress that the isolated zero at $t \approx -1.4$ $(\mathrm{GeV}/c)^2$ of the scattering amplitude without its nearby associate does not necessarily imply a zero of the *t*-eikonal function at a small momentum transfer given by Carvalho and Menon. The existence of the zero at $t \approx -7$ $(\mathrm{GeV}/c)^2$ is the consequence of the observed behavior of the differential cross section, especially at small momentum transfers.

III. A SIMPLE MODEL FOR THE EIKONAL FUNCTION

In the following we examine how the zeros of the *t*-eikonal function affect the zeros of the scattering amplitude. For this purpose we take a model eikonal function

$$\bar{\Omega}(s,t) = F_{\mathrm{z}}^{k} F_{\mathrm{nz}}, \tag{4}$$

where F_{z}^{k} and F_{nz} are the factors having simple zeros and no zeros in the region $-t \geqslant 0$, respectively. For simplicity we take

$$F_{\mathrm{z}}^{k}(s,t) = C^{k}(s) \Pi_{i=1}^{k} (1 - t/\tau_i) \tag{5}$$

and

$$F_{\mathrm{nz}} = (1 - t/\kappa^2)^{-l}. \tag{6}$$

This *t*-eikonal function is a sum of the multipole terms with multiplicity l, $l-1, \ldots, l-k$. Here C^k, τ_i, κ, and l are free parameters to be fixed by the experiment, and it is understood that $F_{\mathrm{z}}^{0}(s,t) = C^{0}$. Here we do not intend to make a quantitative analysis of the experimental data which requires more sophisticated parametrization of the eikonal function than the expression (4), but to clarify the qualitative behavior of the zero trajectories of the scattering amplitude in the total cross-section (σ_{t})–momentum-transfer (t) plane.

We assume $l = 4$ and $\kappa^2 = 0.71$ $(\mathrm{GeV}/c)^2$ of the electromagnetic form factor of the proton, by paying respect to the CY model. For $l = 4$, k is limited to $k \leqslant 3$ to secure the nonsingular behavior of the eikonal function $\Omega(s,b)$. In the following we take only the parameter C^k as energy variant as in the factorized eikonal function model [8], in keeping with the other parameters fixed at the values as prescribed above and below. In reality all parameters would be energy dependent if the formula (4) or a similar expression is used to represent the correct eikonal function, and the effects from the energy variation may deform the zero trajectories, but the essential features of the structure of the trajectories given in the following will be unchanged.

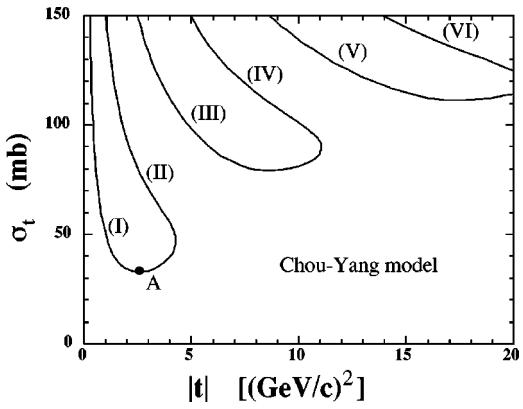

FIG. 1. The zero trajectories of the imaginary part of the scattering amplitude for the $k = 0$ case (the Chou-Yang model).

Case 1: $k = 0$

First we take the case $k = 0$. This is the CY model, of which zero trajectories are first given in Ref. [9] and shown here in Fig. 1. If the total cross section increases, there is a pair creation of dips at $\sigma_{\mathrm{t}} \approx 30$ mb at point A in Fig. 1. For illustrative purposes we assign a number in parentheses to each trajectory as shown in Fig. 1. The behavior of the first trajectory (I) is consistent with the observed dip structure of the pp differential cross section in the ISR energy region and further with the $\bar{p}p$ experimental data of the CERN Super Proton Synchrotron ($\mathrm{S}\bar{p}p\mathrm{S}$) at higher energy. Trajectory (II) is, however, incompatible with the pp experimental data in the ISR energy region without its corresponding dip structure in the experimental data. See Fig. 2 below.

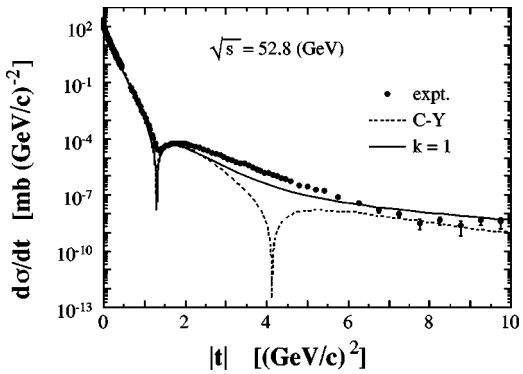

FIG. 2. The differential cross sections of pp scattering at $\sqrt{s} = 52.8$ GeV. The dotted curve represents the $k = 0$ case (the Chou-Yang model), the solid $k = 1$. Here no real part is included.

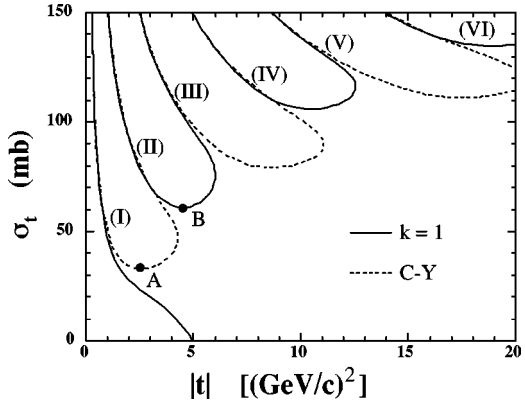

FIG. 3. The zero trajectories of the imaginary part of the scattering amplitude for the $k=1$ case (the solid curve) together with $k=0$ (the Chou-Yang model) (the dotted curve).

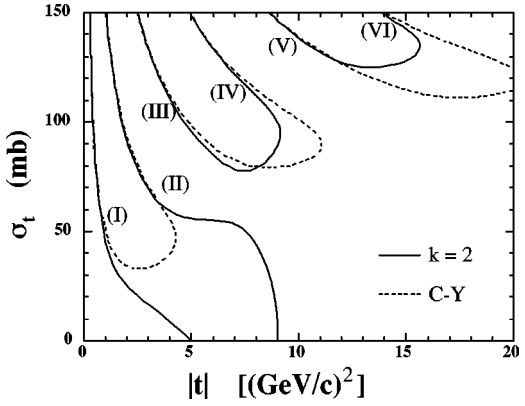

FIG. 4. The zero trajectories of the imaginary part of the scattering amplitude for the $k=2$ case (the solid curve) of $|\tau_2| = 9$ (GeV/c)^2 together with $k=0$ (the Chou-Yang model) (the dotted curve).

Case 2: $k=1$

This difficulty for the behavior of the secondary trajectory (II) can be solved if the t-eikonal function has a zero in the momentum transfer and we examine the t-eikonal function with one zero, $k=1$. We assume $\tau_1=-5.0$ (GeV/c)^2, which roughly reproduces the feature of the differential cross section for the present $F_{\rm nz}$ with $l=4$. We show some examples of the differential cross sections by the CY case ($k=0$) and one-zero case ($k=1$) in Fig. 2 as well as the experimental data of the pp differential cross section at $\sqrt{s}=52.8$ GeV [10]. Here the parameters C^0 and C^1 assumed for these examples give the total cross section $\sigma_{\rm t}=42$ and 38 mb for $k=0$ and 1, respectively. In Fig. 3 we show the zero trajectories for $k=0$ and $k=1$. It can be seen how the zero beginning from the original position $|t|=|\tau_1|=5$ (GeV/c)^2 passes the observed dip position around $|t|=1.4$ (GeV/c)^2 and further flows into trajectory (I) of the CY case as the value of C^1 or the total cross section increases.

It should be remarked that the pair creation of the zero trajectories no longer occurs at point A: instead trajectories (II) and (III) start from point B at $|t|\approx 5$ (GeV/c)^2 around $\sigma_{\rm t}\approx 60$ mb. This is the energy region of S$p\bar{p}$S for $p\bar{p}$ scattering. At $\sqrt{s}=540$ GeV the $p\bar{p}$ experiments have given $\sigma_{\rm t}\approx 60$ mb, but the differential cross section measurements have been performed only in the region $|t|\leqslant 1.6$ (GeV/c)^2 [11]. At higher energy Tevatron experiments have been carried out in the range $|t|\leqslant 0.6$ (GeV/c)^2 at 1800 GeV [12]. Hence the experimental data available at present are very limited in this energy region, and are particularly null in the large momentum transfer region, so we cannot test this prediction of the $k=1$ eikonal function for the pair creation of trajectories (II) and (III).

Case 3: $k=2$

Unlike the pole of the scattering amplitude, the zero has no simple physical significance. The hadron dynamics producing the zero of the t-eikonal function at $t\approx -7$ (GeV/c)^2 [7] is not clear and there is no reason for denying the existence of further zeros. If the pair creation does not occur around point B in Fig. 3 and the second dip appears singly, the t-eikonal function necessitates an additional zero. Such a zero will be able to exist only in the region $|t|>10$ (GeV/c)^2 for consistency with the ISR pp experimental data of the differential cross section measurements.

We show in Figs. 4 and 5 how the second zero would affect the zero trajectories of the scattering amplitude. We give the trajectories for $\tau_2=-9$ and -15 (GeV/c)^2 in Fig. 4 and Fig. 5, respectively. In the cases $\tau_2=-9$ and -15 (GeV/c)^2, the trajectory beginning from τ_2 flows into (II) and (IV), respectively. It is to be noted that for the eikonal function (4) the trajectory starting from $|\tau_2|$ as small as 11 (GeV/c)^2 becomes confluent with (IV). The zero trajectory starting from the second zero of the t-eikonal function never becomes confluent with trajectory (III): this is evident from the behavior of the sign of the scattering amplitude. Trajectory (III) can be created only in pairs with either (II) or (IV).

As the total cross section increases, the zero trajectories of cases $k=1$ and 2 become confluent with those of case $k=0$ which is characterized by the peripheral mass parameter κ. If the experimental measurement is confined to the *small*

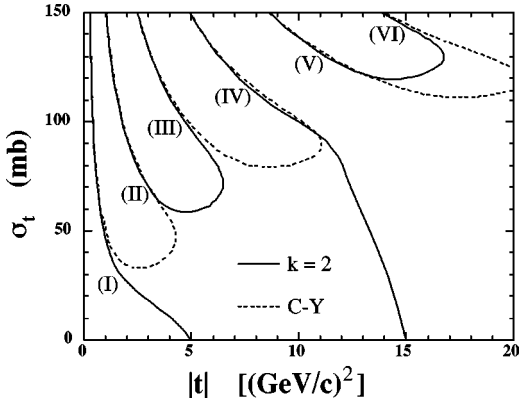

FIG. 5. The zero trajectories of the imaginary part of the scattering amplitude for the $k=2$ case (the solid curve) of $|\tau_2| = 15$ (GeV/c)^2 together with $k=0$ (the Chou-Yang model) (the dotted curve).

momentum-transfer region, for example, $0 \leqslant |t| \leqslant 2$ $(\mathrm{GeV}/c)^2$, the differences of the amplitudes between $k=1$ and $k=2$ are very marginal as can be expected from the distant location of the second zero at τ_2 in the t-eikonal function. The effects of the second zero can be found by performing experiments at large momentum transfers.

IV. MORE REALISTIC MODELS

It is worthwhile to examine the zero trajectories of the amplitudes which better reproduce the differential cross section data than formula (4), since the simple eikonal function (4) reproduces only the gross features of the experimental differential cross section. We show the zero trajectories for the scattering amplitudes which well describe the differential cross section in the ISR energy region. We take the scattering amplitudes referred to as *modified three-exponential* and *multipole* amplitude which have been previously obtained by a phenomenological fit to the pp elastic differential cross section data at $\sqrt{s}=52.8$ GeV [13]. The amplitudes are

$$\mathrm{Im}\,F(s,t)=A_1 e^{B_1 t/2}+A_2 e^{B_2 t/2}-A_3\left[1+c\left(1-\frac{t}{t_0}\right)^2\right]e^{B_3 t/2}, \tag{7}$$

and

$$\mathrm{Im}\,F(s,t)=\overline{A}\left(1-\frac{t}{t_1}\right)\left(1-\frac{t}{t_2}\right)\left(1-\frac{t}{\lambda^2}\right)^{-n}. \tag{8}$$

The eikonal functions at 52.8 GeV are constructed numerically from these two scattering amplitudes and the zero trajectories of the scattering amplitude are evaluated by assuming the energy dependence of the factorized eikonal picture for these eikonals. This implies that we are treating the zeros of the t-eikonal function as energy fixed as in the preceding analysis by formula (4), but its consequences are enough to realize what occurs if the zeros are energy moving.

In addition to these two phenomenological amplitudes, we also take an eikonal model of Bourrely, Soffer, and Wu [6]. We use only the momentum-transfer dependence of the BSW eikonal function as

$$\overline{\Omega}(t)\propto\frac{a^2+t}{a^2-t}\,\frac{1}{(1-t/m_1^2)^2(1-t/m_2^2)^2}, \tag{9}$$

and proceed with a factorized-eikonal analysis.

We show in Fig. 6 the differential cross sections of pp scattering at 52.8 GeV given by these three amplitudes. Here only the contributions from the imaginary part of the scattering amplitude are given. The real part is small at this energy and its main effect is to fill up the discrepancy between the calculated cross sections and the experimental data in the dip region observed in this figure. In the case of the BSW model they have tried to fit the experiments over a wide energy range by a relatively simple form for the eikonal function with a prescribed energy dependence. This seems to cost a fit which is not good at large momentum transfers.

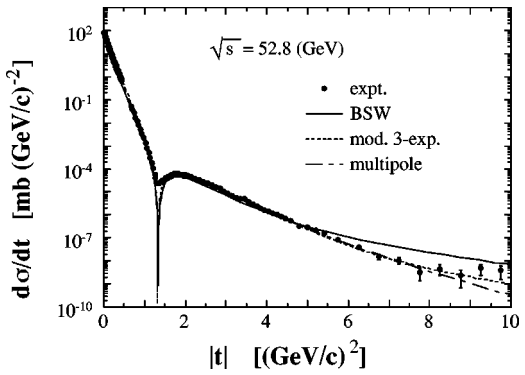

FIG. 6. The differential cross sections of pp scattering at 52.8 GeV by the BSW model (the solid curve) [6], the *modified three-exponential* model (the dotted curve), and the *multipole* model (the dash-dotted curve) [13].

The eikonal functions of the BSW and the *modified three-exponential* amplitude have one zero at $|t|=3.8$ and 7.0 $(\mathrm{GeV}/c)^2$, respectively, while the *multipole* amplitude has two zeros at $|t|=7.6$ and 24.0 $(\mathrm{GeV}/c)^2$. The zero of BSW is located at somewhat small $|t|=3.8$ $(\mathrm{GeV}/c)^2$ in view of the results of Carvalho and Menon, $|t|=7.0\pm2.0$ $(\mathrm{GeV}/c)^2$ [7].

The results for the zero trajectories are given in Fig. 7. There are some significant differences of the behaviors of trajectories (II) and (III) between the case with one zero (the BSW and *modified three exponential* models) and the case with two zeros (the *multipole* model) in the range of total cross section $\sigma_t=60$–90 mb. In the *multipole* case the second zero trajectory starts *singly* from the second zero of the t-eikonal function at a large momentum transfer, $|t|\approx24$ $(\mathrm{GeV}/c)^2$, while trajectories (II) and (III) start by the pair creation around $|t|\approx5$ and 7 $(\mathrm{GeV}/c)^2$ in the BSW and *modified three-exponential* cases, respectively. The fact that in the *multipole* case the second zero trajectory starts from the distant second zero of the t-eikonal function is rather different from the simple model amplitude (4) which produces a zero trajectory flowing into (IV) even for a small $|\tau_2|$ as 11 $(\mathrm{GeV}/c)^2$.

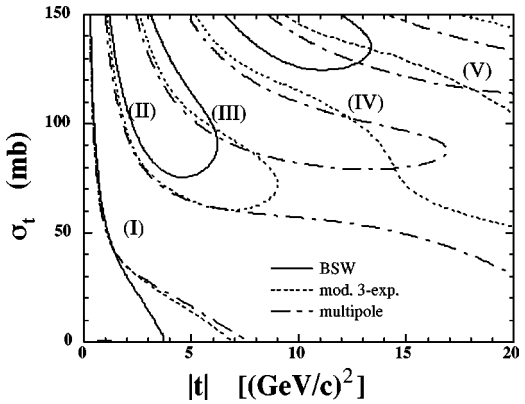

FIG. 7. The zero trajectories of the imaginary part of the scattering amplitude for the BSW model (the solid curve) [6], the *modified three-exponential* model (the dotted curve), and *multipole* model (the dash-dotted curve) [13].

If we compare the *modified three-exponential* and *multipole* models, we can see that both show almost the same zero trajectories and also scattering amplitudes in the range $|t| \leqslant 7$ $(\mathrm{GeV}/c)^2$. This is reasonable since both amplitudes are practically the same in the range $|t| \leqslant 10$ $(\mathrm{GeV}/c)^2$ at 52.8 GeV. At present we cannot predict from the available experimental data of pp and $\bar{p}p$ scattering whether the second zero appears singly or not. It is necessary to perform a measurement of the differential cross section in the wide region of momentum transfer $|t| \leqslant 10$ $(\mathrm{GeV}/c)^2$ in the range of the total cross section $\sigma_t = 60$–90 mb in order to obtain the answer.

There would be some changes in the numerical details in the preceding analysis coming from the uncertainty of the eikonal function, but the basic pattern of the zero trajectories shown in Figs. 1, 3, 4, and 5, and also in Fig. 7, will not be changed essentially [14].

V. ASYMPTOTIC BEHAVIOR OF THE ZERO TRAJECTORIES

In Fig. 7 we can observe how the trajectories of three amplitudes become mutually confluent as the total cross section grows. Asymptotically the elastic hadron-hadron scattering amplitude is considered as becoming a black-disk one [15]. Such a behavior is consistent with the prediction of the axiomatic field theory [16]. In a previous paper we have given an amplitude which has been derived by an asymptotic expansion by utilizing the impact parameter approach and is directly related to the eikonal model [17]. The amplitude has also a close correspondence with the Regge-cut amplitude of Gauron, Nicolescu, and Leader [18]. It is given by

$$\mathrm{Im}\, F \sim R^2 \left\{ \frac{J_1(Rq)}{Rq} \mathrm{Re}\, \Gamma\left(1 + i\frac{q}{\mu}\right) - \frac{J_0(Rq)}{Rq} \mathrm{Im}\, \Gamma\left(1 + i\frac{q}{\mu}\right) \right\}, \tag{10}$$

where J_i is the Bessel function of order i, Γ is the gamma function, q is $\sqrt{-t}$, μ is the mass parameter characterizing the most peripheral part of the diffraction interaction, and R is a length parameter giving the black-disk interaction radius asymptotically. In deriving formula (10) we assume that the eikonal function behaves as

$$\Omega(s,b) \underset{b \to \infty}{\sim} c(s)(\mu b)^n \exp[-(\mu b)], \tag{11}$$

where $c(s)$ is a monotone increasing function of the energy s. The parameter μ is a mass parameter representing the hadronic continuum states responsible for the most peripheral part of the diffraction interaction and its value is bounded from below by twice the pion mass. It is noted that the power n does not appear in these leading terms (10) of the asymptotic expansion [19].

In the amplitude (10) the Bessel functions represent the black-disk structure growing in a central region through the unitarity saturation of the interaction and developing outwards as the energy goes higher, while the gamma functions signify the peripheral departure from the black-disk structure. The similarity of any scattering amplitude to the expression (10) indicates the degree of how the black-disk feature is developed in the amplitude.

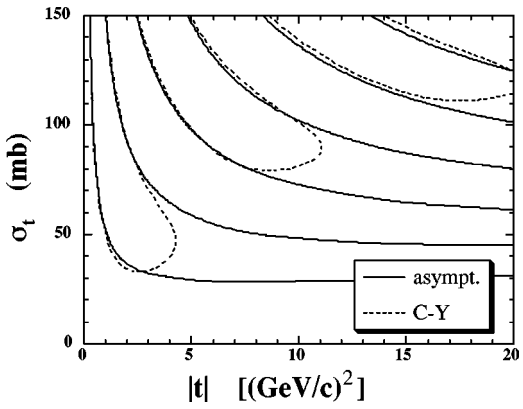

FIG. 8. The zero trajectories of the imaginary part of the scattering amplitude for the asymptotic amplitude (10) with $\mu = 0.6$ GeV (the solid curve) together with the t-eikonal function (4) $k = 0$ (the Chou-Yang model) (the dotted curve).

For the t-eikonal function (4) with (5) and (6) the peripheral behavior is dominated by the factor F_{nz}. The zeros of the t-eikonal function do not affect the asymptotic behavior of the eikonal function and do not produce new trajectories. Any zero trajectory of the scattering amplitude beginning from a zero of the t-eikonal function will flow fast into one of the zero trajectories of the asymptotic amplitude (10) as the total cross section increases. In this respect it will be interesting to compare the zero trajectories of the asymptotic amplitude with the model eikonal function (4). This is given in Fig. 8 where the zero trajectories of the asymptotic amplitude (10) is compared with those of the CY model which is taken as a representative of the eikonal function (4). Here we treat μ as a free parameter rather than taking its asymptotic value $\mu = \kappa$. If we take $\mu = 0.6$ GeV, there is a good confluence of the CY zero trajectories with the asymptotic ones.

VI. REMARKS

We have discussed how the zeros of the scattering amplitude emerge in the hadron-hadron scattering amplitude in terms of the eikonal picture. The behavior of the zero trajectories closely reflects the underlying structure of the diffraction interaction of which we know little theoretically, especially about its short range part. The phenomenological analysis of the currently available experimental data indicates that the t-eikonal function has one zero around $-t \approx 7$ $(\mathrm{GeV}/c)^2$ and there will be probably no further zero in the range $-t \lesssim 20$ $(\mathrm{GeV}/c)^2$. This suggests that there may be at least two components in the diffraction interaction, one with long range and the other with short range. The long range one comes from the inelastic processes realized by the peripheral interactions, but the origin of the short range one is not clear except that it is not produced by the multiple rescattering effects of the former one as far as the eikonal picture is concerned.

For the foreseeable future the possibilities of the experimental investigation of the present problem are the pp ex-

periment at the BNL Relativistic Heavy Ion Collider (RHIC), the $\bar{p}p$ experiment at the FNAL Tevatron, and the pp experiment at the CERN Large Hadron Collider (LHC). The PP2PP experiment at RHIC [20] will produce valuable information for the detailed structure of the diffraction interaction including its spin structure. It is very preferable to extend the project to cover the larger momentum tansfer region $-t > 1.3\ (\mathrm{GeV}/c)^2$. If the behavior of the formation of the second dip in the energy region from RHIC to LHC is clarified, it affords important information to our understanding of the elastic diffraction interaction of hadrons, though it requires difficult experimental works. Such experiments will give much more valuable information for the diffraction interaction rather than to go to higher energies.

[1] See, for example, J. R. Forshaw and D. A. Ross, *Quantum Chromodynamics and the Pomeron*, Cambridge Lectures Notes in Physics, No. 9 (Cambridge University Press, Cambridge, England, 1997).

[2] The real part is induced from the imaginary part by the derivative dispersion relation. See J. B. Bronzan, G. L. Kane, and U. P. Sukhatme, Phys. Lett. **49B**, 227 (1974); J. D. Jackson, in *Proceedings of Fourteenth Scottish Universities Summer School in Physics*, Edinburgh, 1973, edited by R. L. Crawford and R. Jennings (Academic Press, London, 1974), p. 1.

[3] In the region $t \leqslant 0$ and $s \geqslant s_0$ with s_0 as the threshold value, $u = \mathrm{Im}\, F(s,t)$ forms a smooth surface in the (s,t,u) space. The contours of $\mathrm{Im}\, F(s,t) = \mathrm{const}$ are either closed curves or have their end points at the boundaries of the region. This implies that if we meet a *new* zero in t of $\mathrm{Im}\, F(s,t)$ as s increases, it is a double zero which immediately splits into two simple zeros. In the context of the present analysis it is better to use the total cross section σ_{t} instead of the energy-changing parameter which specifies the magnitude of the eikonal function as C^k of Eq. (5), with the understanding that the threshold s_0 corresponds to $\sigma_{\mathrm{t}} = 0$ and $s = \infty$ to $\sigma_{\mathrm{t}} = \infty$, and we look for the behavior of the zero trajectories in the region $\sigma_{\mathrm{t}} \geqslant 0$ and $t \leqslant 0$. The zero trajectories beginning from the boundary $\sigma_{\mathrm{t}} = 0$ stem from the zeros in t of the eikonal function $\bar{\Omega}(s,t)$ persistently existing from the threshold, as we have $\mathrm{Im}\, F(s,t) \approx \bar{\Omega}(s,t)$ for $|\bar{\Omega}(s,t)| \ll 1$.

[4] T. T. Chou and C. N. Yang, Phys. Rev. **170**, 1591 (1968); L. Durand III and R. Lipes, Phys. Rev. Lett. **20**, 637 (1968).

[5] See, for example, T. Maehara, T. Yanagida, and M. Yonezawa, Prog. Theor. Phys. **57**, 1097 (1977).

[6] C. Bourrely, J. Soffer, and T. T. Wu, Nucl. Phys. **B247**, 15 (1984); Z. Phys. C **37**, 369 (1988).

[7] P. A. S. Carvalho and M. J. Menon, Phys. Rev. D **56**, 7321 (1997).

[8] R. Henzi, Nucl. Phys. **B104**, 52 (1976).

[9] T. T. Chou and C. N. Yang, Phys. Rev. Lett. **46**, 764 (1981).

[10] L. Baksay *et al.*, Nucl. Phys. **B141**, 1 (1978); G. Barbiellini *et al.*, Phys. Lett. **39B**, 663 (1972); E. Nagy *et al.*, Nucl. Phys. **B150**, 221 (1979).

[11] UA4 Collaboration, M. Bozzo *et al.*, Phys. Lett. **147B**, 385 (1984); UA4 Collaboration, R. Battiston *et al.*, *ibid.* **127B**, 472 (1983); UA4 Collaboration, M. Bozzo *et al.*, *ibid.* **155B**, 197 (1985).

[12] E-710 Collaboration, N. A. Amos *et al.*, Phys. Lett. B **247**, 127 (1990).

[13] M. Kawasaki, T. Maehara, and M. Yonezawa, Phys. Rev. D **53**, 4838 (1996).

[14] Here we comment on the behavior of the pair of trajectories. One of the pair moves forwards while its associated one moves backwards and then forwards as seen in Fig. 1. This is a typical behavior of the two trajectories created in pair. It is, however, to be noted that in some types of eikonal function the associated one runs backwards nearly flat and turns forwards very slowly or even does not appear to turn forwards, or the pair creation occurs at very large momentum transfer so that two singly created trajectories seem to exist. An example of the latter case is seen in Fig. 7 where trajectories (IV) and (V) for the *modified three-exponential* model (the dotted curve) meet at very large $|t| \approx 39\ (\mathrm{GeV}/c)^2$.

[15] See, for example, M. M. Block and R. N. Cahn, Rev. Mod. Phys. **57**, 563 (1985).

[16] G. Auberson, T. Kinoshita, and A. Martin, Phys. Rev. D **3**, 3185 (1971).

[17] M. Kawasaki, T. Maehara, and M. Yonezawa, Phys. Rev. D **62**, 074005 (2000).

[18] P. Gauron, B. Nicolescu, and E. Leader, Nucl. Phys. **B299**, 640 (1988).

[19] The power n appears in nonleading terms in the asymptotic expansion. This indicates that its effects are important at nonasymptotic energies. The scattering amplitude of any eikonal model having peripheral mass κ can be seen to assume its asymptotic form (10) effectively *earlier* at high, but finite, energies with the parameter $\mu = \kappa - n/R$ which approaches κ asymptotically as R or the total cross section goes infinity.

[20] W. Guryn *et al.*, PP2PP proposal "Total and Differential Cross Sections and Polarization Effects in pp Scattering at RHIC" (unpublished).